https://dx.doi.org/10.22161/ijaers.612.57 *ISSN: 2349-6495(P) | 2456-1908(O)*

Robust Control Applied to a Synchronous Buck Converter with Loss and Uncertainty in its Parameters

Gabriel R. Francisco[1], Umberto X. da S. Neto[2], Eduardo H. Kaneko[3], Matheus F. Mollon[4], Marcio A. F. Montezuma[5]

[1]Undergraduate Student, Universidade Tecnológica Federal do Paraná (UTFPR), Câmpus Cornélio Procópio, Paraná, Brazil
Email: gabrielrossatofrancisco@hotmail.com
[2,3,4]Graduate Student, Universidade Tecnológica Federal do Paraná (UTFPR), Câmpus Cornélio Procópio, Paraná, Brazil
Email:umbertoxavier@gmail.com[2], eduardok@alunos.utfpr.edu.br[3], matheusmollon@alunos.utfpr.edu.br[4]
[5]Department of Mechanical Engineering, Universidade Tecnológica Federal do Paraná (UTFPR), Câmpus Cornélio Procópio, Paraná, Brazil
Email: montezuma@utfpr.edu.br

Abstract**—***This Work presents the application of control with H_∞ problem, together with pole location constraint by LMI formulation in a Buck converter. The uncertainties modeling of the system variables uses the constraint by a convex polytope. Mathematical software with the implementation of algorithms for LMIs solution, as well as software for circuit simulation, were used as an aid for the formulation and validation of the control. The result of the robust controller in a transient period is compared to a classic controller, giving justification for the quality of the results.*

Keywords**—Buck, LMIs, Modeling, Pole Location Constraint, Robust Control.***

I. INTRODUCTION

Direct current to direct current (DC-DC) converters are generally used in many applications due to its ability to increase or decrease voltage with high efficiency. There are several topologies of these converters, one of them is the synchronous buck converter, shown in Fig. 1, which only reduces its input voltage. This when compared to non-synchronous buck has higher efficiency at full load[1]. In order to deliver a near-desired voltage at the output, i.e.a voltage that follows a variable reference, it is essential to use a controller that keeps the system stable to all desired specifications.

The use of linear matrix inequalities (LMIs) has recently been presenting efficient solutions to control problems. This is due to the characteristic of simultaneously considering various requirements, performance constraints and robustness through the formulation of LMIs. In this context, research is growing in several areas, focusing on control through these inequalities [2]. In this work, for example, a robust

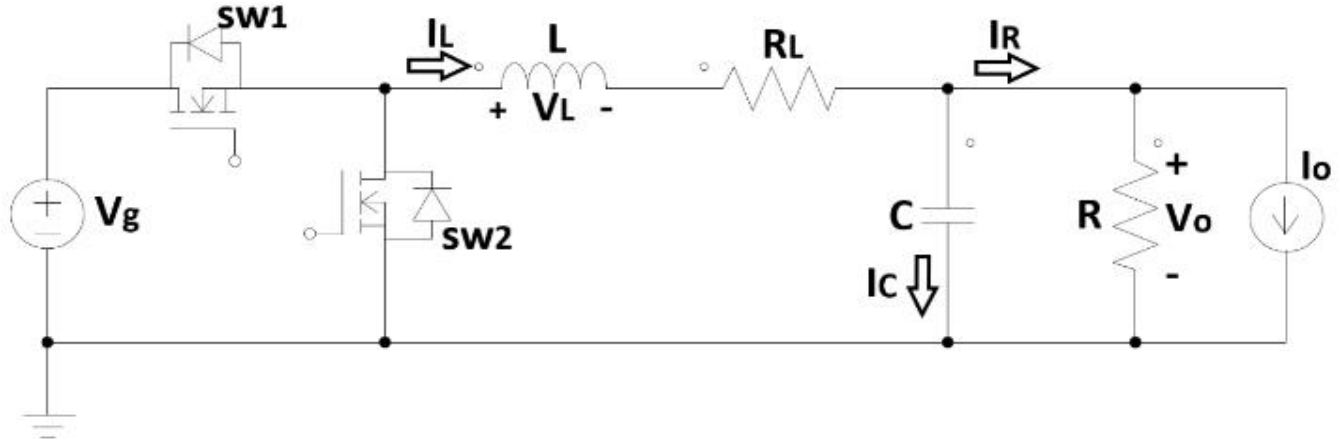

Fig. 1: Synchronous buck converter.

https://dx.doi.org/10.22161/ijaers.612.57 *ISSN: 2349-6495(P) | 2456-1908(O)*

H_∞control is presented, adding constraints on the convex region, in which the closed-loop system poles can be placed. The main reference is the study presented in [3].

To validate this work, two controllers were applied to a DC-DC Buck converter (Fig. 1). TheH_∞control, containing the constraints represented by LMIs, is performed by state feedback. In this way, two sensors are required, one for reading the converter output voltage and one for reading the current over the inductor. The second controller uses the classic approach of Proportional Integral (PI) control. MATLAB/Simulink software was used for system simulation. The SeDuMi, YALMIP and ROLMIP packageswere used in the solution and optimization of the LMIs presented in this work.

The comparison of these two controllers allows us to evaluate the advantage that the H_∞control with pole region constraint considering its characteristic uncertainties, has over the classic PI control. Such a comparison is interesting for three reasons, the first is that the load connected to the converter output may vary within a known range in which the converter is designed to work. The second is that the capacitance may decrease, e.g. an electrolytic capacitor has a liquid dielectric, which may degrade over time. The third is that the real components have tolerances,e.g.$\pm 20\%$, and could vary according to temperature, such as the capacitor and inductor present in the converter.

Finally, the comparison of the results of this work aims to present the differences between a H_∞controller with higher implementation cost, due to the development time and hardware cost, and a PI controller that has a less expressive cost.This paper is divided in the following order. Section II presents the modeling of the Buck converter (Fig. 1). Section III introduces the characteristics of the H_∞controller. Section IV presents the implementation of control techniques and the comparison of results. Section V presents the conclusions.

II. SYSTEM MODELING

Two steps make up the synchronous Buck converter, shown in Fig. 1. On the first step of the switching $SW1$ conducts and $SW2$ shall be open, on the second one $SW2$ conducts and $SW1$ stays open. The duty cycle d represents the portion of the switching period T_S, in which $SW1$ is conducting. The addition of the second load in parallel to the resistance R, represented by the source I_O, represents a disturbance in the output current.

Equating of the inductor voltage to each switching step and its weighting of the values by switching parcel results in (1) and (2). The equating of the capacitor current to each switching step, following the same weighting, results in (3) and (4):

$$< V_L > = \frac{1}{T_S}.\Big(\big(V_g - V_O - R_L.I_L\big).d.T_S + (-V_O - R_L.I_L).(1-d).T_S\Big) \quad (1)$$

$$< \boldsymbol{V_L} > = L.\frac{\boldsymbol{dI_L}}{\boldsymbol{dt}} = \boldsymbol{V_g}.\boldsymbol{d} - \boldsymbol{V_O} - \boldsymbol{R_L}.\boldsymbol{I_L} \quad (2)$$

$$< I_C > = \frac{1}{T_S}.\left(\left(I_L - \frac{V_O}{R} - I_O\right).d.T_S + \left(I_L - \frac{V_O}{R} - I_O\right).(1-d).T_S\right) \quad (3)$$

$$< \boldsymbol{I_C} >= \boldsymbol{C}.\frac{\boldsymbol{dV_O}}{\boldsymbol{dt}} = \boldsymbol{I_L} - \frac{\boldsymbol{V_O}}{\boldsymbol{R}} - \boldsymbol{I_O} \quad (4)$$

From (2) and (4), it is possible to perform alternating current(AC) modeling for small signals. In this, the average values summed to an AC portion replace each variable. The DC terms that represent the permanent response cancel each other. Moreover, it is assumed that the second order AC terms are small compared to the first order ones, to the extent that you can neglectthem [4]. Such process is presented in (5) to (13).

$$V_g = \overline{V_g} + \widehat{V_g} \quad (5)$$

$$V_O = \overline{V_O} + \widehat{V_O} \quad (6)$$

$$I_L = \overline{I_L} + \widehat{I_L} \quad (7)$$

$$I_O = \overline{I_O} + \widehat{I_O} \quad (8)$$

$$d = \bar{d} + \hat{d} \quad (9)$$

$$L.\frac{d\big(\overline{I_L} + \widehat{I_L}\big)}{dt} = \overline{V_g}.\bar{d} + \overline{V_g}.\hat{d} + \widehat{V_g}.\bar{d} + \widehat{V_g}.\hat{d} - \overline{V_O} - \widehat{V_O} - R_L.\overline{I_L} - R_L.\widehat{I_L} \quad (10)$$

$$\boldsymbol{L}.\frac{\boldsymbol{d\big(\widehat{I_L}\big)}}{\boldsymbol{dt}} = \boldsymbol{\overline{V_g}}.\boldsymbol{\hat{d}} + \boldsymbol{\widehat{V_g}}.\boldsymbol{\bar{d}} - \boldsymbol{\widehat{V_O}} - \boldsymbol{R_L}.\boldsymbol{\widehat{I_L}} \quad (11)$$

$$C.\frac{d(\overline{V_O} + \widehat{V_O})}{dt} = \overline{I_L} + \widehat{I_L} - \frac{\overline{V_O}}{R} - \frac{\overline{\widehat{V_O}}}{R} - \overline{I_O} - \widehat{I_O} \quad (12)$$

$$\boldsymbol{C}.\frac{\boldsymbol{d(\widehat{V_O})}}{\boldsymbol{dt}} = \boldsymbol{\widehat{I_L}} - \frac{\boldsymbol{\overline{\widehat{V_O}}}}{\boldsymbol{R}} - \boldsymbol{\widehat{I_O}} \quad (13)$$

The model given by (11) and (13) is a type 0, i.e. the plant has no integrator. For the steady-state system error to be null, for a ramp type input, it is necessary to insert an integrator augmented state, shown in (14) and (15). This transforms the system into type 1 [5].

$$x_3 = \int \big(V_{ref} - \widehat{V_O}\big).dt \quad (14)$$

$$\frac{\boldsymbol{d(x_3)}}{\boldsymbol{dt}} = \boldsymbol{V_{ref}} - \boldsymbol{\widehat{V_O}} \quad (15)$$

Considering (11), (13) and (15), it is possible to represent them in state space notation, as presented in (16) and (17):

$$\frac{dx(t)}{dt} = A.x(t) + B_u.u(t) + B_w.w(t) + B_{ref}.V_{ref}. \quad (16)$$

$$z(t) = C_z.x(t) + D_{zu}.u(t) + D_{zw}.w(t) \quad (17)$$

, wherein:

https://dx.doi.org/10.22161/ijaers.612.57 *ISSN: 2349-6495(P) | 2456-1908(O)*

$$x(t) = \begin{bmatrix} \widehat{I_L} \\ \widehat{V_O} \\ x_3 \end{bmatrix} \quad \ldots\ldots (18)$$

$$u(t) = \left[\hat{d}\right] \quad \ldots\ldots (19)$$

$$w(t) = \left[\widehat{I_O}\right] \quad \ldots\ldots (20)$$

$$z(t) = \left[\widehat{V_O}\right] \quad \ldots\ldots (21)$$

$$A = \begin{bmatrix} -\frac{R_L}{L} & -\frac{1}{L} & 0 \\ \frac{1}{C} & -\frac{1}{R.C} & 0 \\ 0 & -1 & 0 \end{bmatrix} \quad \ldots\ldots (22)$$

$$B_u = \begin{bmatrix} \frac{\overline{V_g}}{L} \\ 0 \\ 0 \end{bmatrix} \quad \ldots\ldots (23)$$

$$B_w = \begin{bmatrix} 0 \\ -\frac{1}{C} \\ 0 \end{bmatrix} \quad \ldots\ldots (24)$$

$$B_{ref} = \begin{bmatrix} 0 \\ 0 \\ 1 \end{bmatrix} \quad \ldots\ldots (25)$$

$$C_z = [0 \quad 1 \quad 0] \quad \ldots\ldots (26)$$

$$D_{zw} = [0] \quad \ldots\ldots (27)$$

$$D_{zu} = [0] \quad \ldots\ldots (28)$$

The disturbance represented by the w vector, from the current source $\widehat{I_O}$, represents the behavior of the converter output voltage V_O, for sudden changes in the output current of the converter[3]. The parameters $\overline{V_g}$, L, C e R are uncertain and limited to a minimum and maximum value, as represented by (29) to (32):

$$\beta = \overline{V_g} \in \left[\overline{V_g}_{mim}, \overline{V_g}_{max}\right] \quad \ldots\ldots (29)$$

$$\delta = \frac{1}{L} \in \left[\frac{1}{L_{max}}, \frac{1}{L_{min}}\right] \quad \ldots\ldots (30)$$

$$\psi = \frac{1}{C} \in \left[\frac{1}{C_{max}}, \frac{1}{C_{min}}\right] \quad \ldots\ldots (31)$$

$$\mu = \frac{1}{R.C} \in \left[\frac{1}{C_{max}.R_{max}}, \frac{1}{C_{min}.R_{min}}\right] \quad \ldots\ldots (32)$$

Therefore, matrices A and B_u depend on these $N = 4$ uncertain parameters, generating a polytope with $2^N = 16$ vertices. Table 1 shows the polytopic representation of matrices A and B_u.

III. ROBUST CONTROL CHARACTERISTICS

This Section presents the characteristics of the robust H_∞ control developed in this paper.

3.1 LMIs

Considering $x \in \mathbb{R}^m$ as the variable and $F_i = F_i{}'$ as non-variant matrices. An LMI has the form given in (33):

$$F(x) \triangleq F_0 + \sum_{i=1}^{m} F_i x_i > 0 \quad \ldots\ldots (33)$$

According to [6], there is an LMI feasibility problem when a solution x has to be found, such that $F(x) > 0$.

The analysis of LMIs in dynamic systems has over a century of study, beginning in 1890, when Lyapunov's theory was published. This theory shows that a differential equation, given in (34), is stable, if and only if, there is a positive definite matrix P, which satisfies (35):

$$\frac{d}{dt}x(t) = Ax(t) \quad \ldots\ldots (34)$$

$$A'P + PA < 0 \quad \ldots\ldots (35)$$

Lyapunov proved that for the LMI in (35) to have a solution $P > 0$, one must choose any matrix $Q > 0$ and solve the equation $A'P + PA + Q = 0$. If $P > 0$ is found, there is a solution [2].

The sequence of studies on LMIs showed that the classic LQR (Linear Quadratic Regulator) problem, associated with the Riccati equation, could be represented as an LMI problem, through the Schur complement [2]. This verification is important because, if possible, several problems can be solved together, if represented in LMI form, as shown in (36) with k constraints.

$$F(x) = diag\{F_0(x), F_1(x), \ldots, F_k(x)\} > 0 \quad \ldots\ldots (36)$$

Over time, several algorithms have been developed for the solution and optimization of LMIs, such as Nemirovskii's algorithm [2]. Today, with computational packages, LMIs have become an efficient tool in many engineering areas, including modern control [7].

3.2 Quadratic stability

The existence of a quadratic function, given in (37), that satisfies $\dot{V}(x) < 0$, is a necessary and sufficient condition to assume that the linear system, presented in (34), is stable. Thus resulting in (38):

$$V(x) = x'Px > 0, \quad \forall x \neq 0 \quad \ldots\ldots (37)$$

$$\dot{V}(x) = x'(A'P + PA)x < 0, \quad \forall x \neq 0 \quad \ldots\ldots (38)$$

Then, the system is stable, if and only if, there is a positive definite symmetric matrix P, for which $\dot{V}(x) < 0$. To satisfy (38), the conditions in (39) must be met:

$$\exists P > 0 \; ; \quad A'P + PA < 0 \quad \ldots\ldots (39)$$

If the uncertainties in A are polytopic, the feasibility of the LMI problem must be verified, i.e. the polytope must have j vertices. Then, a $P > 0$ solution must be found, such that (40) is met:

$$A_i{}'P + PA_i < 0, \quad i = 1,2, \ldots, j \quad \ldots\ldots (40)$$

The feasibility of this problem implies that the system is stable for every matrix belonging to the polytope.

https://dx.doi.org/10.22161/ijaers.612.57 *ISSN: 2349-6495(P) | 2456-1908(O)*

Table 1: Polytopic representation of matrices A and B_u.

$A_1 = \begin{bmatrix} -\frac{R_L}{L_{min}} & -\frac{1}{L_{min}} & 0 \\ \frac{1}{C_{min}} & -\frac{1}{R_{min}.C_{min}} & 0 \\ 0 & -1 & 0 \end{bmatrix}$, $B_{u_1} = \begin{bmatrix} \frac{\overline{V_g}_{mim}}{L_{min}} \\ 0 \\ 0 \end{bmatrix}$	$A_9 = \begin{bmatrix} -\frac{R_L}{L_{max}} & -\frac{1}{L_{max}} & 0 \\ \frac{1}{C_{min}} & -\frac{1}{R_{min}.C_{min}} & 0 \\ 0 & -1 & 0 \end{bmatrix}$, $B_{u_9} = \begin{bmatrix} \frac{\overline{V_g}_{mim}}{L_{max}} \\ 0 \\ 0 \end{bmatrix}$
$A_2 = \begin{bmatrix} -\frac{R_L}{L_{min}} & -\frac{1}{L_{min}} & 0 \\ \frac{1}{C_{max}} & -\frac{1}{R_{min}.C_{max}} & 0 \\ 0 & -1 & 0 \end{bmatrix}$, $B_{u_2} = \begin{bmatrix} \frac{\overline{V_g}_{mim}}{L_{min}} \\ 0 \\ 0 \end{bmatrix}$	$A_{10} = \begin{bmatrix} -\frac{R_L}{L_{max}} & -\frac{1}{L_{max}} & 0 \\ \frac{1}{C_{max}} & -\frac{1}{R_{min}.C_{max}} & 0 \\ 0 & -1 & 0 \end{bmatrix}$, $B_{u_{10}} = \begin{bmatrix} \frac{\overline{V_g}_{mim}}{L_{max}} \\ 0 \\ 0 \end{bmatrix}$
$A_3 = \begin{bmatrix} -\frac{R_L}{L_{min}} & -\frac{1}{L_{min}} & 0 \\ \frac{1}{C_{min}} & -\frac{1}{R_{max}.C_{min}} & 0 \\ 0 & -1 & 0 \end{bmatrix}$, $B_{u_3} = \begin{bmatrix} \frac{\overline{V_g}_{mim}}{L_{min}} \\ 0 \\ 0 \end{bmatrix}$	$A_{11} = \begin{bmatrix} -\frac{R_L}{L_{max}} & -\frac{1}{L_{max}} & 0 \\ \frac{1}{C_{min}} & -\frac{1}{R_{max}.C_{min}} & 0 \\ 0 & -1 & 0 \end{bmatrix}$, $B_{u_{11}} = \begin{bmatrix} \frac{\overline{V_g}_{mim}}{L_{max}} \\ 0 \\ 0 \end{bmatrix}$
$A_4 = \begin{bmatrix} -\frac{R_L}{L_{min}} & -\frac{1}{L_{min}} & 0 \\ \frac{1}{C_{max}} & -\frac{1}{R_{max}.C_{max}} & 0 \\ 0 & -1 & 0 \end{bmatrix}$, $B_{u_4} = \begin{bmatrix} \frac{\overline{V_g}_{mim}}{L_{min}} \\ 0 \\ 0 \end{bmatrix}$	$A_{12} = \begin{bmatrix} -\frac{R_L}{L_{max}} & -\frac{1}{L_{max}} & 0 \\ \frac{1}{C_{max}} & -\frac{1}{R_{max}.C_{max}} & 0 \\ 0 & -1 & 0 \end{bmatrix}$, $B_{u_{12}} = \begin{bmatrix} \frac{\overline{V_g}_{mim}}{L_{max}} \\ 0 \\ 0 \end{bmatrix}$
$A_5 = \begin{bmatrix} -\frac{R_L}{L_{min}} & -\frac{1}{L_{min}} & 0 \\ \frac{1}{C_{min}} & -\frac{1}{R_{min}.C_{min}} & 0 \\ 0 & -1 & 0 \end{bmatrix}$, $B_{u_5} = \begin{bmatrix} \frac{\overline{V_g}_{max}}{L_{min}} \\ 0 \\ 0 \end{bmatrix}$	$A_{13} = \begin{bmatrix} -\frac{R_L}{L_{max}} & -\frac{1}{L_{max}} & 0 \\ \frac{1}{C_{min}} & -\frac{1}{R_{min}.C_{min}} & 0 \\ 0 & -1 & 0 \end{bmatrix}$, $B_{u_{13}} = \begin{bmatrix} \frac{\overline{V_g}_{max}}{L_{max}} \\ 0 \\ 0 \end{bmatrix}$
$A_6 = \begin{bmatrix} -\frac{R_L}{L_{min}} & -\frac{1}{L_{min}} & 0 \\ \frac{1}{C_{max}} & -\frac{1}{R_{min}.C_{max}} & 0 \\ 0 & -1 & 0 \end{bmatrix}$, $B_{u_6} = \begin{bmatrix} \frac{\overline{V_g}_{max}}{L_{min}} \\ 0 \\ 0 \end{bmatrix}$	$A_{14} = \begin{bmatrix} -\frac{R_L}{L_{max}} & -\frac{1}{L_{max}} & 0 \\ \frac{1}{C_{max}} & -\frac{1}{R_{min}.C_{max}} & 0 \\ 0 & -1 & 0 \end{bmatrix}$, $B_{u_{14}} = \begin{bmatrix} \frac{\overline{V_g}_{max}}{L_{max}} \\ 0 \\ 0 \end{bmatrix}$
$A_7 = \begin{bmatrix} -\frac{R_L}{L_{min}} & -\frac{1}{L_{min}} & 0 \\ \frac{1}{C_{min}} & -\frac{1}{R_{max}.C_{min}} & 0 \\ 0 & -1 & 0 \end{bmatrix}$, $B_{u_7} = \begin{bmatrix} \frac{\overline{V_g}_{max}}{L_{min}} \\ 0 \\ 0 \end{bmatrix}$	$A_{15} = \begin{bmatrix} -\frac{R_L}{L_{max}} & -\frac{1}{L_{max}} & 0 \\ \frac{1}{C_{min}} & -\frac{1}{R_{max}.C_{min}} & 0 \\ 0 & -1 & 0 \end{bmatrix}$, $B_{u_{15}} = \begin{bmatrix} \frac{\overline{V_g}_{max}}{L_{max}} \\ 0 \\ 0 \end{bmatrix}$
$A_8 = \begin{bmatrix} -\frac{R_L}{L_{min}} & -\frac{1}{L_{min}} & 0 \\ \frac{1}{C_{max}} & -\frac{1}{R_{max}.C_{max}} & 0 \\ 0 & -1 & 0 \end{bmatrix}$, $B_{u_8} = \begin{bmatrix} \frac{\overline{V_g}_{max}}{L_{min}} \\ 0 \\ 0 \end{bmatrix}$	$A_{16} = \begin{bmatrix} -\frac{R_L}{L_{max}} & -\frac{1}{L_{max}} & 0 \\ \frac{1}{C_{max}} & -\frac{1}{R_{max}.C_{max}} & 0 \\ 0 & -1 & 0 \end{bmatrix}$, $B_{u_{16}} = \begin{bmatrix} \frac{\overline{V_g}_{max}}{L_{max}} \\ 0 \\ 0 \end{bmatrix}$

3.3 Quadratic stability for a closed-loop system with state feedback

The LMIs in (39) are adapted for a closed-loop system with state feedback $u = Kx$. Works [3] and [8] simplify these LMIs using the following theorem:

Theorem 3.1: The closed-loop system with state feedback $u = Kx$ is stable, if and only if, there is a symmetric matrix$W \in \mathbb{R}^{nxn}$and a matrix$Y \in \mathbb{R}^{mxn}$, such that:

$W > 0$ ..... (41)

$AW + WA' + B_uY + Y'B_u{}' < 0$ ..... (42)

The state feedback gain is obtained by (43):

$K = YW^{-1}$ ..... (43)

3.4 Pole placement

The main motivation for pole clustering, in a specific region on the left side of the complex plane, is the transient response characteristics of a linear system. A second order system, e.g. with poles $-\zeta w_n \pm jw_d$, is fully characterized in terms of the undamped natural frequency$w_n = |\lambda|$, the damping rateζ and the damped natural frequency$w_d = w_n\sqrt{1-\zeta^2}$.By constraining and fixing λ in a prescribed region, bounds can be put on the characteristic values, thus ensuring a satisfactory transient response. The regions of interest, that can be defined, include theα-stability regions vertical strips, disks, conic sectors, $(Re(s) \leq -\alpha)$, and others [9].

The prominent region of this project, which has control purposes, is characterized by the set $S(\alpha, \rho, \theta)$, composed of complex numbers $\sigma + jw_d$, that satisfy (44) [9]:

$\sigma < -\alpha < 0; \quad |\sigma + jw_d| < \rho; \quad tan\theta\sigma < -|w_d|$ (44)

https://dx.doi.org/10.22161/ijaers.612.57 *ISSN: 2349-6495(P) | 2456-1908(O)*

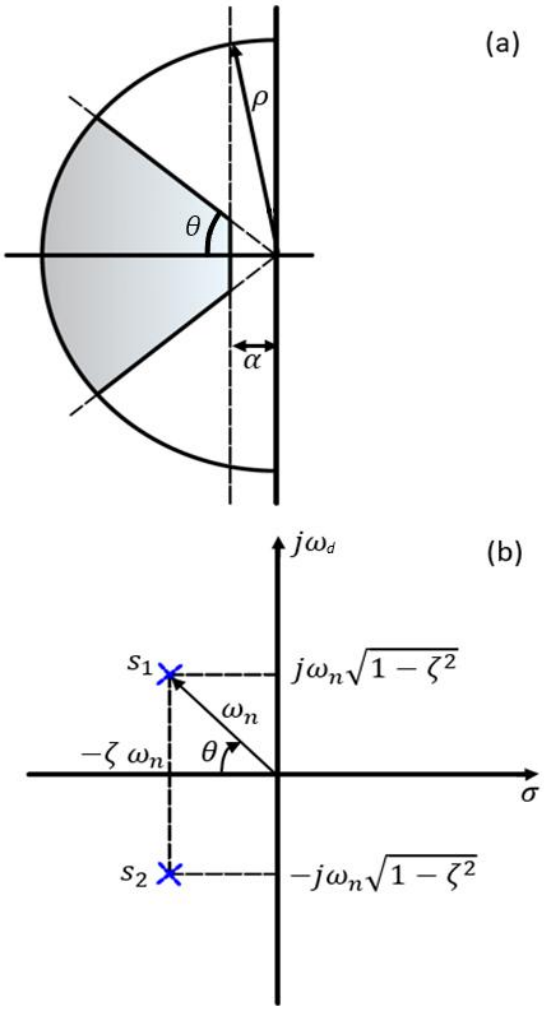

Fig. 2: Pole region constraint geometry [9].

Fig. 2 (a) demonstrates the set S and its variables.The comparison of Fig. 2 (a) and Fig. 2 (b) relates certain parameters of a control system, such as the minimum decay rate$\alpha = \zeta w_n$, the minimum damping ratio$\zeta = cos\theta$, and the maximum undamped natural frequency$w_d = \rho.sen$.Setting the minimum or maximum characteristics of each parameterbounds the maximum overshoot, delay time, rise time and settling time [9].

From [9] a study is made for the representation of the constraint, presented in Fig. 2 (a), by means of LMIs. Works [3] and [8] simplify these LMIs by the following theorem:

Theorem 3.2: The closed-loop poles of a system, considering the state feedback control law $u = Kx$, are within the region defined by the set$S(\alpha, r, \theta)$, if there is a positive symmetric matrix$W$and a matrix$Y$, such that:

$$AW + WA' + B_uY + Y'B'_u + 2\alpha W < 0 \quad \ldots\ldots\ldots\ldots (45)$$

$$\begin{bmatrix} -\rho W & WA' + Y'B'_u \\ AW + B_uY & -\rho W \end{bmatrix} < 0 \quad \ldots\ldots\ldots\ldots\ldots\ldots (46)$$

$$\begin{bmatrix} sen\theta(AW + WA' + B_uY + Y'B'_u) & cos\theta(AW - WA' + B_uY - Y'B'_u) \\ cos\theta(-AW + WA' - B_uY + Y'B'_u) & sen\theta(AW + WA' + B_uY + Y'B'_u) \end{bmatrix} < 0 \quad \ldots\ldots (47)$$

O ganho de realimentação de estados é dado por (48):

$$K = YW^{-1} \quad \ldots\ldots\ldots\ldots\ldots\ldots\ldots\ldots\ldots\ldots\ldots\ldots\ldots\ldots\ldots\ldots (48)$$

3.5 TheH_∞ norm

TheH_∞norm can be represented by the H_2 norm, being equivalent to the largest value obtained by this one.Therefore, considering the$\mathcal{G}$ operatorsbelonging to theH_∞ space, (49) is defined:

$$\|\mathcal{G}\|_\infty = sup_{x\in\mathcal{L}_2} \frac{\|\mathcal{G}_x\|_2}{\|x\|_2} = sup_{\|x\|_2=1} \|\mathcal{G}_x\|_2 \quad \ldots\ldots\ldots (49)$$

If the operator is a transfer function$G(s)$, the definition in (50) can be used:

$$\|G\|_\infty = sup_w \bar{\sigma}\{G(j\omega)\} \quad \ldots\ldots\ldots\ldots\ldots\ldots\ldots\ldots\ldots\ldots (50)$$

Considering that$\bar{\sigma}\{G(jw)\}$is the maximum singular value of$G(j\omega)$. If$G(s)$ isa SISO (Single Input and Single Output) transfer function, theH_∞ normcorresponds to the largest value of the Bode diagram, for example.

TheH_∞ problemconsists of finding a controller, such that theH_∞norm of the closed-loop transfer function G_{wz} (where$w$is the disturbance and$z$is the output) is minimized, i.e. less than a specified valueγ.This value being determined using a particular case of the small gain theorem.

The work [2] explains how to calculate the H_∞norm for a closed-loop system with state feedback, determining the dual system LMIs, presented by [10] using the following theorem:

Theorem 3.3: A closed-loop system with state feedback$u = Kx$ and$\frac{\|Z\|_2}{\|w\|_2} < \gamma$, is stable,if and only if, there is a positive defined symmetric matrix$W \in \mathbb{R}^{nxn}$and a matrix$Y \in \mathbb{R}^{mxn}$, such that:

$$\begin{bmatrix} AW + WA' + B_uY + Y'B'_u & B_w & WC'_z + Y'D_{zu} \\ B'_w & -\gamma I & D'_{zw} \\ C_zW + D_{zu}Y & D_{zw} & -\gamma I \end{bmatrix} < 0 \quad \ldots (51)$$

The constraint proposed in (41) and (42) is included in (51), so Theorem 3.3 ensures quadratic stability.

IV. SIMULATION RESULTS

The model obtained in Section II for the Buck converter does not take into account its switching frequency $f_s = 100kHz$. In order to prevent the control from destabilizing, it is necessary to limit the maximum bandwidth of the controller to a frequency 10 times lower than the switching frequency [3].

The purpose of the H_∞control is to have a maximum overshoot of 20% ($\%Over$) and a minimum settling time

https://dx.doi.org/10.22161/ijaers.612.57 *ISSN: 2349-6495(P) | 2456-1908(O)*

of 10ms (T_e). The parameters α, θ e ρcan be related to the desired system performance through (52) to (55) [5].

$$\xi = \frac{-log(\%Over/100)}{\sqrt{\pi^2 + log(\%Over/100)^2}} = 0{,}45595 \ldots\ldots\ldots (52)$$

$$\theta = arcos(\xi) = 62{,}8739° \ldots\ldots\ldots\ldots\ldots\ldots\ldots\ldots (53)$$

$$\alpha = \frac{4}{\xi . T_e} = 877.28 \ldots\ldots\ldots\ldots\ldots\ldots\ldots\ldots\ldots\ldots\ldots (54)$$

$$\rho = 2.\pi.\frac{f_S}{10} = 62831.85 \ldots\ldots\ldots\ldots\ldots\ldots\ldots\ldots\ldots\ldots (55)$$

The synchronous Buck converter always operates similar to the continuous conduction mode, since its switches do not depend on the current flowing in the inductor to polarize, as it does in the non-synchronous converter's diode [1].For any R load, there is a peak-to-peak output voltage ripple of $\Delta V_o = 12{,}5mV$, and in the inductor there is a peak-to-peak current ripple equivalent to$\Delta I_L = 500mA$.

Such ripples are the result of the switching process, and the maximum values are defined in the converter design.The controller itself cannot mitigate these ripples. For the converter operating at steady state, the minimum values of the inductor$L$and capacitor$C$are defined according to (56) and (57). In these, the duty cycle$D = 0.5$is where the largest ripples of current and voltage occur [11]. The inductor Lin practice is not ideal as it has a fixed resistanceR_L.

$$L_{min} = \frac{\bar{V}_{g_{max}} . D . (1 - D)}{\Delta I_L . f_S} \ldots\ldots\ldots\ldots\ldots\ldots\ldots\ldots\ldots\ldots (56)$$

$$C_{min} = \frac{\bar{V}_{g_{max}} . D . (1 - D)}{8 . L_{min} . \Delta V_o . f_S^2} \ldots\ldots\ldots\ldots\ldots\ldots\ldots\ldots\ldots\ldots (57)$$

The values range of the DC-DC Buck converter uncertain parameters is shown in Table 2.

Table 2: DC-DC Buck converter parameters.

Parameters	Values Range
R_L	$0.1\ \Omega$
L	$[500, 800]\mu H$
C	$[50, 200]\mu F$
R	$[2, 100]k\Omega$
V_g	$[80, 100]V$

Using MATLAB, the converter system, described in (16) and (17), with its polytopic representation of 16 vertices, shown in Table 1, was implemented for the parameter ranges presented in Table 2.With the aid of the SeDuMi, YALMIP and ROLMIP packages, the LMIs, represented by (41), (45), (46), (47) and (51), were optimized.As a result, the state feedback gain, in (58), was obtained. The gamma minimization resulted in$\gamma = 4.0809$. The block diagram representation, built with MATLAB/Simulink, of the Buck converter with state feedback control, is shown in Fig. 3.

$$K = [0.3389 \quad -0.4435 \quad 603.6809] \ldots\ldots\ldots\ldots\ldots (58)$$

The PI controller was designed, for comparison, with the parameters presented in Table 3. As a result, the proportional and integral gains are shown, respectively, in (59) and (60).

Table 3: PI control design parameters.

Parameters	Values
Margem de Fase	45.5950°
f_c	$558\ Hz$
L	$650\ \mu H$
C	$125\ \mu F$
R	$5\ k\Omega$
V_g	$90\ V$

$$K_P = 3.5951 \times 10^{-4} \ldots\ldots\ldots\ldots\ldots\ldots\ldots\ldots\ldots\ldots\ldots (59)$$

$$K_I = 1.1827 \ldots\ldots\ldots\ldots\ldots\ldots\ldots\ldots\ldots\ldots\ldots\ldots\ldots (60)$$

To evaluate the response of the implemented controllers, five test scenarios were defined. In the first one, the performance of the controllers was compared, without considering the uncertainties in the Buck converter parameters.In this scenario, the voltage reference was a step signal equivalent to$V_{ref} = 60\ V$at the initial time, and changed to$V_{ref} = 30\ V$ after$0.05\ s$. The output voltages obtained for the robust and PI controllers are shown in Fig. 4.

https://dx.doi.org/10.22161/ijaers.612.57 *ISSN: 2349-6495(P) | 2456-1908(O)*

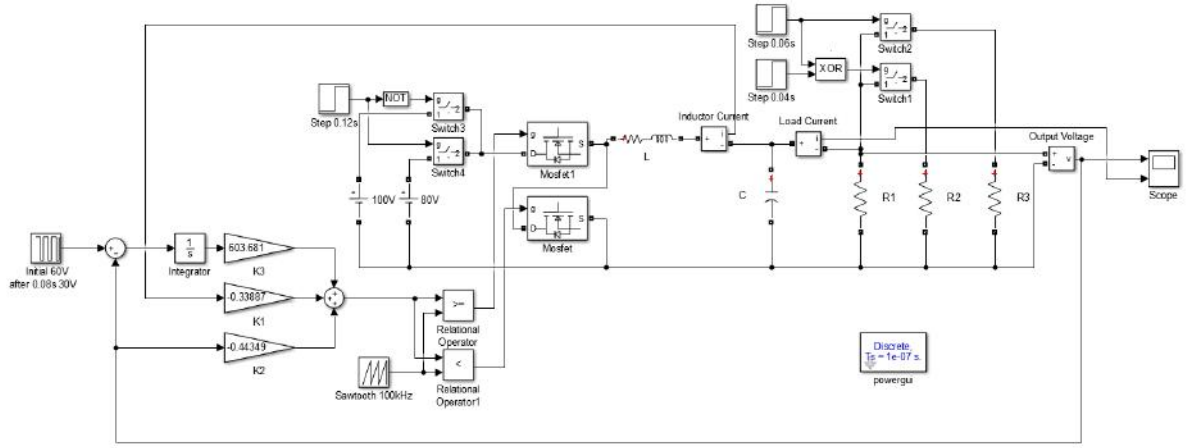

Fig. 3: Synchronous Buck converter with state feedback control.

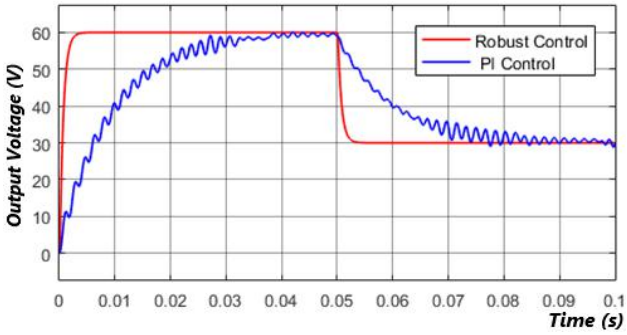

Fig. 4: Converter output voltage scenario 1.

The next four test scenarios evaluated the system response considering the uncertainties in the system parameters.The voltage reference was a step signal equivalent to $V_{ref} = 60\,V$ at the initial time, and changed to $V_{ref} = 30\,V$ after $0.08\,s$. The voltage input was a step signal equivalent to $V_g = 100\,V$ at the initial time, and changed to $V_g = 80\,V$ after $0.12\,s$. The load R also varied, initially it was$R = 100\,k\Omega$, changing to $R = 2\,\Omega$attime$0.04\,s$, and to$R = 10\,\Omega$attime$0.06\,s$. These settings were used for the test scenarios 2, 3, 4, and 5.

Considering the values range of the DC-DC Buck converter uncertain parameters, shown in Table 2, the scenario 2 converter was configured with inductance $L = 500\,uH$and capacitance$C = 50\,uF$. Fig. 5 compares the scenario 2 control responses.

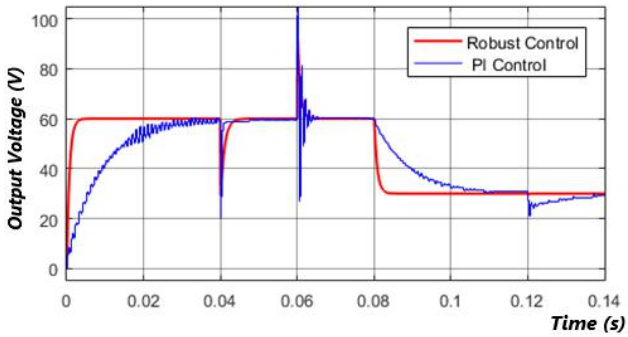

Fig. 5: Converter output voltagescenario 2.

The scenario 3 converter was configured with inductance $L = 500\,uH$ and capacitance $C = 200\,uF$. Fig. 6 compares the scenario 3 control responses.

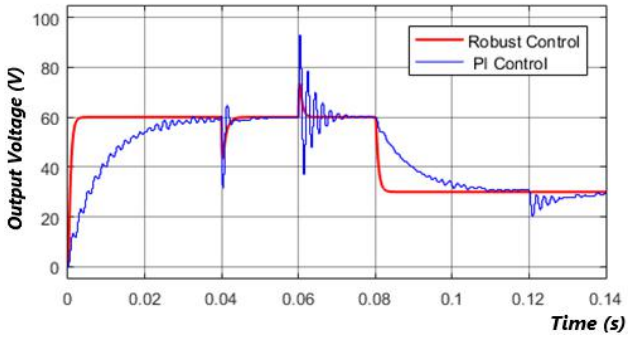

Fig. 6: Converter output voltage scenario 3.

The scenario 4 converter was configured with inductance $L = 800\,uH$ and capacitance $C = 50\,uF$. Fig. 7 compares the scenario 4 control responses.

https://dx.doi.org/10.22161/ijaers.612.57 *ISSN: 2349-6495(P) | 2456-1908(O)*

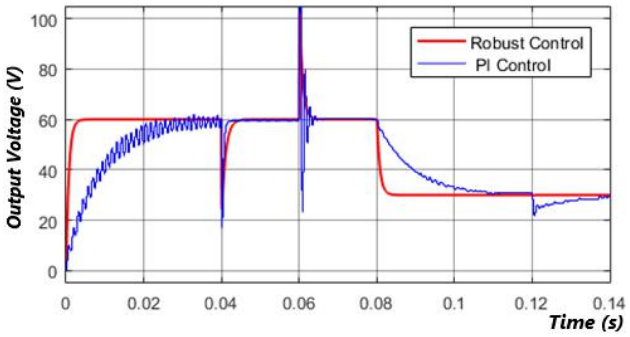

Fig. 7: Converter output voltage scenario 4.

The scenario 5 converter was configured with inductance $L = 800\ uH$ and capacitance $C = 200\ uF$. Fig. 8 compares the scenario 5 control responses.

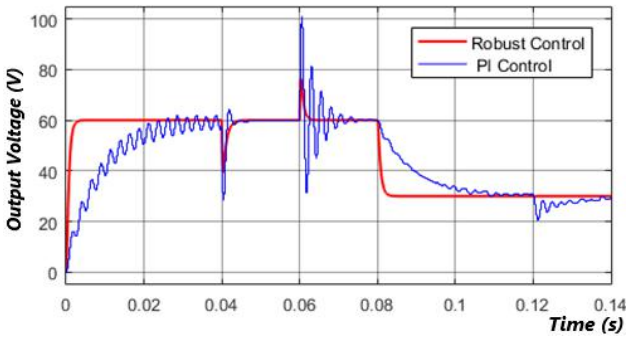

Fig. 8: Converter output voltage scenario 5.

It can be observed in Figs. 5 to 8 that for all the uncertainties considered in the design, the proposed robust controller was stable and within the desired performance conditions. The robust controller presented satisfactory transient responses to the R step loads and the applied input voltage V_g, in comparison to the classic PI controller operating outside its nominal design range.

V. CONCLUSION

The set of linear matrix inequalities (LMIs) presented in this work allows us to ensure robustness and closed-loop poles placement within the desired region, for any state space modeled system. In this work, a Synchronous Buck converter was modeled and a state feedback gain, obtained from the LMIs optimization, was applied. The system's robustness and the desired performance were observed through simulation.

The proposed robust controller achieved a more consistent performance over the adopted parameters range, in comparison to the classic PI control. As can be observed when the output loads are changed, and a step signal is applied to the converter's input voltage, for the minimum and maximum values of the adopted inductance and capacitance ranges.

ACKNOWLEDGEMENTS

Acknowledgements are directed to the Capes Foundation for the material and financial support, which made possible the accomplishment of this work.

REFERENCES

[1] R. Nowakowski and N. Tang. (2009). Efficiency of synchronous versus nonsynchronous buck converters. Retrieved from: https://e2echina.ti.com/cfs-file/__key/telligent-evolution-components-attachments/13-112-00-00-00-00-58-17/Efficiency-of-synchronous-versus-nonsynchronous-buck-converters.pdf.

[2] C. A. R. Crusius, Formulação LMI para problemas de performance e robustez, M.S. thesis, UFSC, May, 1996.

[3] C. Olalla, R.Leyva, A. El Aroudi, P.Garcés and I. Queinnec, LMI robust control design for boost PWM convertes, IET Power Eletronics, vol.3, iss.1, pp.75-85, 2010.

[4] R. Erickson, Fundamentals of Power Electronics, 2nd ed. New Jersey: Kluwer Academinc Publishers, 2000.

[5] K. Ogata, Engenharia de controle moderno, 5th ed. São Paulo, SP: Pearson Prentice Hall, c2010.

[6] S. Boyd, L. El Ghaoui and E. Feron, V. Balakrishnan, Linear matrix inequalities in system and control theory, Society for Industrial and Applied Mathematics, Philadelphia: SIAM,vol. 15, 1994.

[7] A. Trofino, Apostila para a disciplina de controle robusto da pós-graduação da engenharia elétrica da Universidade Federal de Santa Catarina, August, 2000.

[8] L.P.Sampaio and S.A.O.Silva, Robustcontrol applied to photovoltaic array emulator using buck converter, International Conference on Renewable Energies and Power Quality, vol.1, no.13, pp.665-670, April 2015.

[9] M. Chilali and P. Gahinet, H∞ design with pole placement constraints: an LMI approach, IEEE Transactions on Automatic Control, vol. 41, no. 3, pp. 358-367, March 1996

[10] P.Gahinet, P. Apkarian, A linear matrix inequality approach to H∞control, International Journal of Robust and Nonlinear Control, vol.4, pp. 421-448, April 1994.

[11] I. Barbi and D. C. Martins, Eletrônica de potência: conversores CC-CC básicos não isolados, 2nd ed. Florianópolis: Ed. do Autor, 2006.